

Insight into band alignment of Zn(O,S)/CZTSe solar cell by simulation

Zhen-Wu Jiang(姜振武), Shou-Shuai Gao(高守帅), Si-Yu Wang(王思宇), Dong-Xiao Wang(王东潇), Peng Gao(高鹏), Qiang Sun(孙强), Zhi-Qiang Zhou(周志强), Wei Liu(刘玮), Yun Sun(孙云), Yi Zhang(张毅)

Citation: Chin. Phys. B . 2019, 28(4): 048801. **doi:** 10.1088/1674-1056/28/4/048801
Journal homepage: http://cpb.iphy.ac.cn; http://iopscience.iop.org/cpb

What follows is a list of articles you may be interested in

Effect of carrier mobility on performance of perovskite solar cells

Yi-Fan Gu(顾一帆), Hui-Jing Du(杜会静), Nan-Nan Li(李楠楠), Lei Yang(杨蕾), Chun-Yu Zhou(周春宇)
Chin. Phys. B . 2019, 28(4): 048802. **doi:** 10.1088/1674-1056/28/4/048802

Discovery and design of lithium battery materials via high-throughput modeling

Xuelong Wang(王雪龙), Ruijuan Xiao(肖睿娟), Hong Li(李泓), Liquan Chen(陈立泉)
Chin. Phys. B . 2018, 27(12): 128801. **doi:** 10.1088/1674-1056/27/12/128801

Potentials of classical force fields for interactions between Na^+ and carbon nanotubes

De-Yuan Li(李德远), Guo-Sheng Shi(石国升), Feng Hong(洪峰), Hai-Ping Fang(方海平)
Chin. Phys. B . 2018, 27(9): 098801. **doi:** 10.1088/1674-1056/27/9/098801

Promise of commercialization: Carbon materials for low-cost perovskite solar cells

Yu Cai(蔡宇), Lusheng Liang(梁禄生), Peng Gao(高鹏)
Chin. Phys. B . 2018, 27(1): 018805. **doi:** 10.1088/1674-1056/27/1/018805

420 nm thick $CH_3NH_3PbI_{3-x}Br_x$ capping layers for efficient TiO_2 nanorod array perovskite solar cells

Long Li(李龙), Cheng-Wu Shi(史成武), Xin-Lian Deng(邓新莲), Yan-Qing Wang(王艳青), Guan-Nan Xiao(肖冠南), Ling-Ling Ni(倪玲玲)
Chin. Phys. B . 2018, 27(1): 018804. **doi:** 10.1088/1674-1056/27/1/018804

Insight into band alignment of Zn(O,S)/CZTSe solar cell by simulation*

Zhen-Wu Jiang(姜振武)[1], Shou-Shuai Gao(高守帅)[1], Si-Yu Wang(王思宇)[1], Dong-Xiao Wang(王东潇)[1], Peng Gao(高鹏)[2], Qiang Sun(孙强)[2], Zhi-Qiang Zhou(周志强)[1], Wei Liu(刘玮)[1], Yun Sun(孙云)[1], and Yi Zhang(张毅)[1,†]

[1] *Institute of Photoelectronic Thin Film Devices and Technology, Tianjin Key Laboratory of Photoelectronic Thin Film Devices and Technology, Tianjin* 300071, *China*
[2] *Tianjin Institute of Power Source, Tianjin* 300384, *China*

(Received 6 January 2019; revised manuscript received 31 January 2019; published online 5 March 2019)

Cd-free kesterite structured solar cells are currently attracting attention because they are environmentally friendly. It is reported that Zn(O,S) can be used as a buffer layer in these solar cells. However, the band alignment is not clear and the carrier concentration of Zn(O,S) layer is low. In this study, the band alignment of the Zn(O,S)/$Cu_2ZnSnSe_4$ p–n junction solar cell and the effect of In_2S_3/Zn(O,S) double buffer layer are studied by numerically simulation with wxAMPS software. By optimizing the band gap structure between Zn(O,S) buffer layer and $Cu_2ZnSnSe_4$ absorber layer and enhancing the carrier concentration of Zn(O,S) layer, the device efficiency can be improved greatly. The value of CBO is in a range of 0 eV–0.4 eV for S/(S + O)= 0.6–0.8 in Zn(O,S). The In_2S_3 is mainly used to increase the carrier concentration when it is used as a buffer layer together with Zn(O,S).

Keywords: CZTSe, band alignment, double buffer layer, simulation

PACS: 88.40.H–, 88.30.gg, 88.40.hj, 88.40.jn **DOI:** 10.1088/1674-1056/28/4/048801

1. Introduction

Kesterite structured Cu_2ZnSnS_4 (CZTS) and $Cu_2ZnSnSe_4$ (CZTSe) materials have received extensive attention due to their non-toxicity, large absorption coefficient ($> 10^4$ cm^2), and earth abundant component elements in earth.[1–7] Up to now, the champion efficiency of $Cu_2ZnSn(S,Se)_4$ (CZTSSe) solar cell with CdS buffer has reached to 12.6%.[8] For pure selenide CZTSe device, the device performance has been improved to 11.6% with CdS serving as a buffer layer.[9] However, the CdS buffer layer is a potential risk for CIGS and CZTS(e) solar cells[10–12] since the cadmium in CdS is toxic and the band gap of CdS is low (2.4 eV), which will cause the absorption to lose in a short-wavelength region.

Owing to these disadvantages, alternative buffer materials are used to replace the CdS buffer layer. Among them, Zn(O,S) is a promising alternative material due to its non-toxicity and large band gap which can be modified from 2.6 eV to 3.8 eV, depending on the S/(S + O) ratio in Zn(O,S).[13,14] Many groups have reported the kesterite structure-based device with Zn(O,S) serving as a buffer layer. Among them, Grenet *et al.* have reported that the barrier at the CZTSSe/Zn(O,S) interface decreased after light soaking treatment, and the device efficiency was increased to 5.8%.[15] Neuschitzer *et al.* optimized the band alignment between CZTSe absorber layer and Zn(O,S) buffer layer by changing the thiourea concentration in the CBD process. The device efficiency was increased up to 6.5% which was close to that of CdS reference device.[16] Recently, our group eliminated the secondary phases existing in the as-grown Zn(O,S) by sequential concentrated ammonium solution etching and low temperature annealing treatment. Finally, the Zn(O,S)/CZTSe efficiency was increased to 7.2% by our group recently.[17] However, we found that the band offset between Zn(O,S) and CZTSe is higher than 1 eV, which is very difficult for the carrier transport. After the temperature-dependent *I–V* study, we deduce that the carrier transport in such a system should be realized by a defect energy level close to Fermi level which acts as a shortcut for the carrier transport.

The performance of the Zn(O,S)/CZTSe device also suffers the low conductivity.[18,19] The efficiency of the device is seriously deteriorated with low buffer carrier concentration. The most commonly used method to enhance the carrier concentration is element doping. Many groups have improved the carrier concentration of the TCO by doping the group III elements like indium into ZnO.[20–23] Indium acts as a dopant since it has a similar atomic radius to Zn^{2+}. It can substitute Zn^{2+} in ZnO to form In^{+}_{Zn} substitution, which is an n-type dope for ZnO.[24] Recently, Jani *et al.* have doped different concentrations of indium into Zn(O,S) layer by the spray deposition

*Project supported by the National Natural Science Foundation of China (Grant Nos. 51572132, 61674082, and 61774089), the National Key Research and Development Program of China (Grant No. 2018YFB1500202), the Tianjin Natural Science Foundation of Key Project of China (Grant Nos. 16JCZDJC30700 and 18JCZDJC31200), and the 111 Project, China (Grant No. B16027).

†Corresponding author. E-mail: yizhang@nankai.edu.cn

© 2019 Chinese Physical Society and IOP Publishing Ltd

method.[25] The carrier concentration of Zn(O,S) was significantly enhanced by doping 1 wt%–3 wt% indium. The electrical conductivity was improved due to the formation of In^{+}_{Zn} substitution and reduction of hydroxyl group in the Zn(O,S) by annealing treatment in argon atmosphere.[25] Later, Mitzi *et al.* used In_2S_3/CdS double buffer layer in the traditional CZTSSe solar cells. The indium could diffuse into both CdS buffer layer and CZTSSe absorber layer by rapid thermal annealing treatment. Since the atomic radius of indium was similar to that of cadmium in CdS and that of tin in CZTSSe, indium could substitute cadmium and tin and form In_{Cd} and In_{Sn} substitution. Consequently, the carrier concentration of buffer layer and absorber layer were enhanced due to the formation of n-type doping and p-type doping, respectively.[26] Ikeda *et al.* used the In_2S_3 as a buffer layer and they also reported that the CZTS carrier concentration was increased after rapid post-heat treatment.[27]

Kesterite structured solar cells with Zn(O,S) have made considerable progress. However, the study of detailed understanding of the CZTSe/Zn(O,S) is still rare. In this study, we investigate the band alignment between Zn(O,S) layer and CZTSe layer. The effect of the carrier concentration variation in the buffer on the performance of CZTSe solar cells is also studied. We find that double buffer layer In_2S_3/Zn(O,S) mainly increases the carrier concentration.

2. Numerical modeling

The devices are simulated by wxAMPS software, which is updated from the original AMPS program.[28] Based on the main physical principles of AMPS, the wxAMPS software induces two new tunneling models and improves the algorithm by combining the Newton method and the Gummel method. Compared with other simulation software, the wxAMPS provides a good stability and running speed, and is very suitable for simulating materials with defect densities, band tails.[29] The device parameters used in the simulation process are listed in Table 1. The temperature and the illumination spectrum are set to be 300 K and AM1.5, respectively.

Table 1. Device parameters used in simulation.

Parameters	Al:ZnO	In_2S_3	Zn(O,S)	CZTSe
Thickness/nm	500	variable	20	1500
Permittivity	9	13.5	9	8
Band gap energy/eV	3.3	2.1–2.9	2.6–3.8	1
Electron affinity/eV	4.3	4.65-3.85	3.4–4.6	4.35
Carrier concentration/cm^{-3}	1×10^{18}	1×10^{17}	variable	1×10^{16}
Electron mobility/(cm^2/V·s)	100	400	75	40
Holes mobility/(cm^2/V·s)	25	210	20	10
Conduction band effective density of states/cm^{-3}	2.2×10^{18}	1.8×10^{19}	2.2×10^{18}	2.2×10^{18}
Valance band effective density of states/cm^{-3}	1.8×10^{19}	4×10^{13}	1.8×10^{19}	1.8×10^{19}
Defect concentration/cm^{-3}	1×10^{17}	1.7×10^{16}	1×10^{18}	1×10^{14}

3. Results and discussion

3.1. S/(S + O) ratio in Zn(O,S)

The band gap of Zn(O,S) can be adjusted from 2.6 eV to 3.8 eV by modifying the S/(S + O) ratio.[13,14] Sharbati S *et al.* reported that the band gap of the Zn(O,S) first decreases and then increases, and the value of the conduction band and the valence band both change with S fraction variety in the Zn(O,S).[30] The variation of electron affinity (χ_e) and band gap energy (E_g) with S ratio $x = S/(S+O)$ in $Zn(O_{1-x}S_x)$ can be approximately calculated from the following equations:[13,31]

$$E_{gZn(O,S)}(x) = xE_{gZnS} + (1-x)E_{gZnO} - b(1-x)x, \quad (1)$$

$$\chi_e = 4.48 + 0.88x - 1.92x^2, \quad (2)$$

where x is the S fraction, E_g is the band gap, and the band gap value of ZnS and ZnO are 3.6 eV and 3.2 eV, respectively, and b is the bowing factor, which is about 3. Figure 1 shows the corresponding values and variation tendencies of E_g and χ_e with different S/(S + O) ratios. Obviously, the minimum band gap appears in the region where the S and O fraction are almost equal. The value of E_g increases no matter whether the S fraction is higher or lower than 0.5.

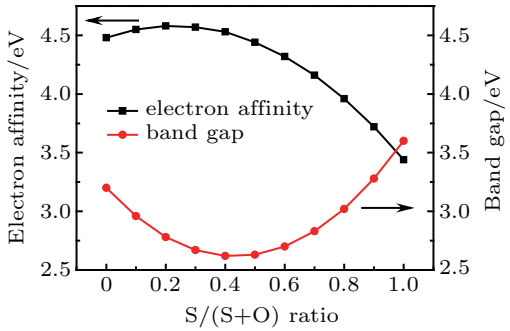


Fig. 1. Electron affinity and band gap energy of Zn(O,S) *versus* S/(S + O) ratio.

As the band gap and the electron affinity of Zn(O,S) vary with the S fraction,[32] the S/(S + O) ratio becomes a key factor to affect the conduction band offset (CBO) at the interface between CZTSe absorber layer and Zn(O,S) buffer layer.[31] The Zn(O,S) electron affinity tends to slide downward as the

S fraction increases (Fig. 1). So the CBO between CZTSe and Zn(O,S) is negative when the buffer layer has a lower S content ($x \leq 0.5$) which is named the cliff-like band alignment. In this case, the CZTSe conduction band edge is higher than that of Zn(O,S), the recombination in the CZTSe/Zn(O,S) interface increases.[33,34] As a result, the FF and V_{oc} become undesirable, and the performance of the device will deteriorate. In contrast, the CBO in the CZTSe/Zn(O,S) interface is spike-like alignment when the S fraction is higher than 0.5 ($x > 0.5$). Too large a CBO will induce a barrier that hinders the photo-generated electrons from transferring across the interface, resulting in J_{sc} decreasing. However, when the value of CBO is set to be in a range from 0 eV to 0.4 eV, the negative effect of the spike-like CBO is negligible.[33,34]

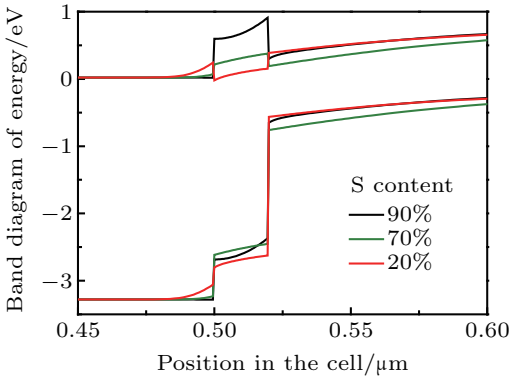


Fig. 2. Band alignments of Zn(O,S)/CZTSe devices with different S fractions.

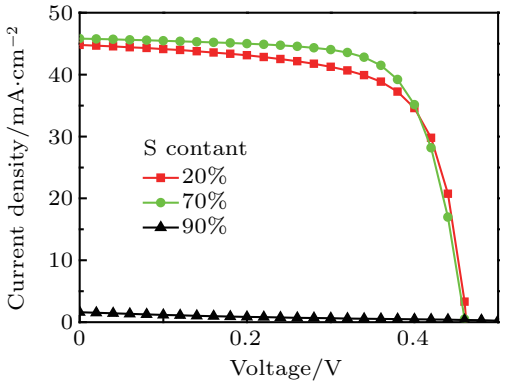


Fig. 3. *J*–*V* curves of Zn(O,S)/CZTSe devices with different S fractions.

Figure 2 shows the band structures of the CZTSe/Zn(O,S) device with different S/(S + O) ratios ($x = 0.2$, 0.7, 0.9). The thickness of the Zn(O,S) used in simulation is 20 nm. The value of CBO at CZTSe/Zn(O,S) interface changes from negative to positive with the increase of S content. As the S fraction increases in Zn(O,S), the barrier induced by large CBO becomes higher.[31] From Fig. 3, when x is 0.9, the CBO is far beyond 0.4 eV, which is considered to be difficult for electron to flow across the interface. We can see that when the S content is higher than 0.7, the *J*–*V* characteristic curve of device is damaged due to the large barrier for photo-generated electrons. In our simulation process, the optimal S content appears at 0.7, and in this case, the CBO between CZTSe and Zn(O,S) is about +0.2 eV, which is in a reasonable range(0 eV–0.4 eV).[33,34] The performance of the device is improved due to the small CBO value at the interface and high light absorption.

3.2. Thickness of Zn(O,S)

The optimal band gap of Zn(O,S) simulation (2.8 eV) is larger than that of CdS (2.4 eV). Consequently, the absorption loss in the short-wavelength region of the visible spectrum is reduced by using the Zn(O,S) film to replace the traditional CdS buffer material, thus improving the short circuit current of the device. The EQE responses of the devices with different buffer layers (CdS layer and Zn(O,S) layer) are showed in Fig. 4. The short wavelength response of device is obviously improved by replacing the CdS layer with Zn(O,S) layer. Figure 5 shows the band structures of solar cells with different Zn(O,S) thickness values for the S/(S + O) = 0.7. Neuschitzer *et al.* have fabricated a 6.5% efficient CBD-Zn(O,S)/CZTSe device after light soaking treatment,[16] while their CBD-Zn(O,S) was less than 10 nm in thickness. According to the results reported previously, too thin a buffer layer can induce pinholes and shunt channels which deteriorate the device parameters. Meanwhile, as the carrier concentration of the untreated CBD-Zn(O,S) is usually low,[18,19] the barrier of the carrier transport will become higher with the thickness of the Zn(O,S) increasing.

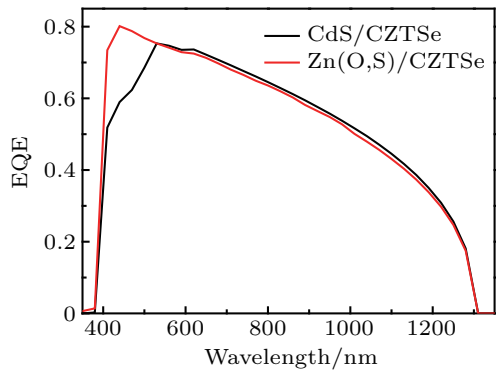


Fig. 4. EQE responses to wave of devices with different buffer layers.

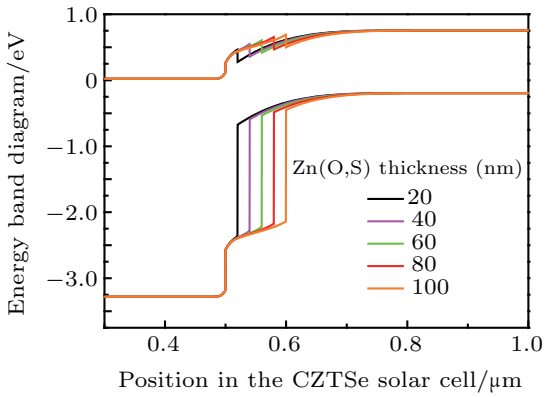


Fig. 5. Energy band structure diagram of Zn(O,S)/CZTSe devices for various Zn(O,S) layer thickness.

Figure 6 shows the variation of the short circuit current density (J_{sc}) and fill factor (FF) with the Zn(O,S) thickness increase. This demonstrates that the J_{sc} and FF dramatically collapse as the Zn(O,S) thickness increases when the carrier concentration of Zn(O,S) is low (5×10^{17} cm^{-3}). However, the performance of the device is almost constant when the carrier concentration is adequately high (5×10^{18} cm^{-3}). This phenomenon is due to the low buffer carrier concentration, leading to the undesirable conductivity in Zn(O,S) layer.[19] However, it will become serious when Zn(O,S) film is thicker. This indicates that the effect of thickness is dependent on the Zn(O,S) carrier concentration.

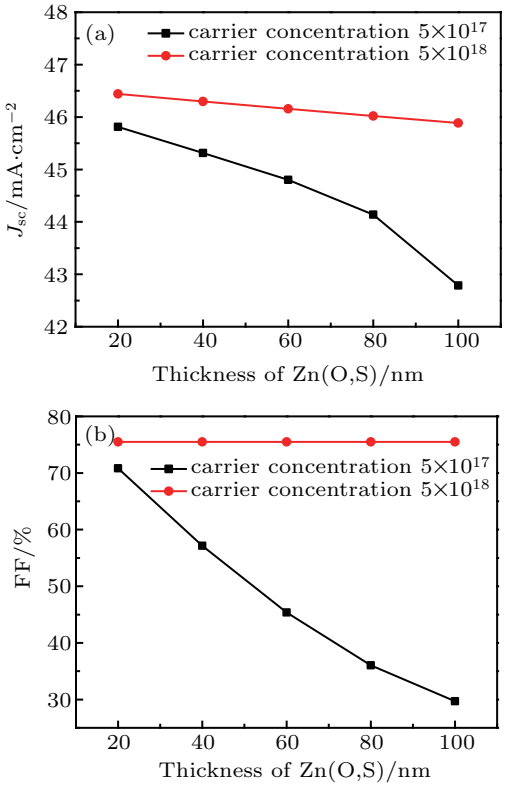


Fig. 6. Curves of (a) J_{sc} and (b) FF of Zn(O,S)/CZTSe solar cells *versus* Zn(O,S) layer thickness with different Zn(O,S) carrier concentrations.

Similarly, we can see from Fig. 7(a) that the poor conductivity makes the photo-generated electrons hard to collect by the buffer layer in the case of constant Zn(O,S) layer thickness when the carrier concentration of Zn(O,S) layer is low. The recombination rate increases in the absorber region as thickness increases. Thus the J_{sc} and FF are deteriorated seriously respectively as the thickness reaches to 100 nm. From Fig. 7(b), when the carrier concentration is as high as 5×10^{18} cm^{-3}, the recombination rate in absorber layer is low and unchanged with the thickness of Zn(O,S) layer. As the photo-generated carrier is mainly generated at CZTSe absorber layer, the recombination rate at the buffer layer has almost no effect on the device performance, so the variation of J_{sc} and FF caused by the variable thickness are negligible. To reduce the light absorption in the buffer layer, the thickness of Zn(O,S) should not be too thick. To ensure that the absorber layer is completely covered, the optimum Zn(O,S) thickness is 20 nm in our simulation, which accords with our previous experiment result.[17] Besides, we find that the effect of buffer thickness depends on carrier concentration of the buffer. The high carrier concentration is propitious to the device performance.

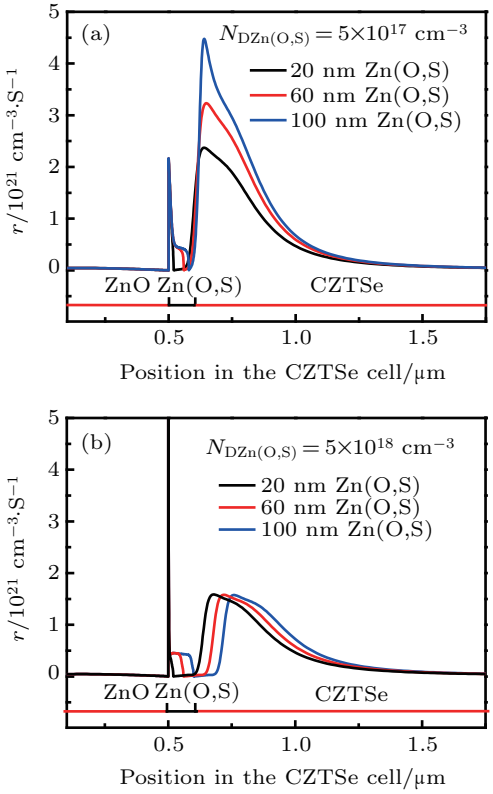


Fig. 7. Recombination rates of Zn(O,S)/CZTSe devices with different Zn(O,S) thickness and carrier concentrations of Zn(O,S) of (a) 5×10^{17} cm^{-3}, (b) 5×10^{18} cm^{-3}.

3.3. Double buffer layer

The In_2S_3/Zn(O,S) double buffer layer is selected for simulation. Obviously, In^{3+} ions will diffuse into Zn(O,S) buffer layer. As a consequence, the carrier concentration of Zn(O,S) is improved due to the dopant of the n-type In^{+}_{Zn}. Thus, we first try to disclose the effect of In_2S_3/Zn(O,S) double buffer layer on carrier concentration On the assumption that the In_2S_3 layer is ultrathin, it diffuses into Zn(O,S) layer completely. Figure 8 shows the conduction band alignment of Zn(O,S)/CZTSe heterojunction with different Zn(O,S) carrier concentrations. According to the simulation results and our previous experimental result,[17] the thickness of Zn(O,S) is set to be 20 nm., The distance from Fermi level to the conduction band minimum when carrier concentration is high (5×10^{18} cm^{-3}) is greater than that when the carrier concentration of Zn(O,S) is as low as 1×10^{16} cm^{-3}. Relatively, the barrier at the interface of Zn(O,S)/CZTSe is high without doping, which impedes the photo-generated electrons flowing across the interface. With the increase of the carrier concentration, the barrier height be-

comes lower. The parameters of Zn(O,S)/CZTSe solar cells with different Zn(O,S) carrier concentrations are listed in Table 2, demonstrating that the performance of the device is observed to improve as the carrier concentration increases due to the forming of the In^{+}_{Zn} substitutions in Zn(O,S) layer.

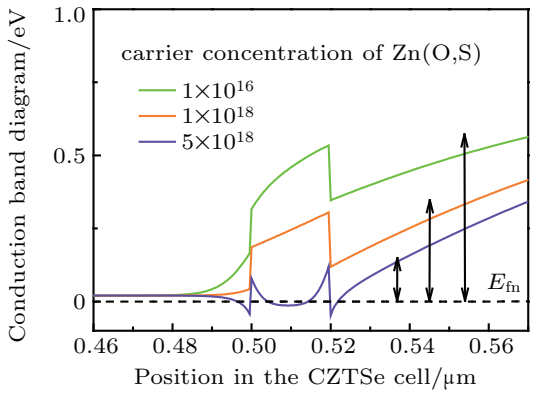


Fig. 8. Conduction band alignments of Zn(O,S)/CZTSe devices with different Zn(O,S) carrier concentrations.

Table 2. Performances of Zn(O,S)/CZTSe cells with different Zn(O,S) carrier concentrations.

Carrier concentration/cm^{-3}	J_{sc}/(mA/cm^2)	V_{oc}/mV	FF/%	Efficiency/%
1×10^{16}	45.5	461	55.8	11.72
1×10^{18}	45.9	461	74.9	15.89
5×10^{18}	46.4	462	75.50	16.18

Some In_2S_3 layers ineluctably remain on the surface of Zn(O,S)/CZTSe solar cell in experiment. The effect of residual In_2S_3 layers should be further considered. The band gap of In_2S_3 is tunable from 2.1 eV to 2.9 eV, which should be attributed to the variation of the temperature and the oxygen content doped into the In_2S_3 layer.[35–37] Furthermore, the electron affinity of In_2S_3 will change with the variation of band gap.[38] The relationship between the band gap and electron affinity is shown below.[38]

$$E_g = 6.75 - \chi_e. \tag{3}$$

The optimal band gap (2.83 eV) and electron affinity (4.16 eV) of Zn(O,S) are fixed. The properties of Zn(O,S) layer and CZTSe absorber layer keep constant in this simulation. The χ_e range of In_2S_3 varies from 3.85 eV to 4.65 eV. The band gap of In_2S_3 layer is larger (2.8 eV–2.9 eV) or smaller (2.1 eV–2.8 eV) than that of Zn(O,S) layer. To make clear the effect of In_2S_3/Zn(O,S) double buffer layer and ensure that the incident light is fully absorbed by CZTSe solar cell, the In_2S_3 layer with a band gap of 2.9 eV should be deposited on the absorber layer and the In_2S_3 layer with a band gap of 2.1 eV–2.8 eV should be deposited between the absorber layer and Zn(O,S) layer. And the thickness of the remaining In_2S_3 layer is set to be 5 nm. Figure 9 shows the *J*–*V* curve of Zn(O,S)/CZTSe device with and without 2.9-eV In_2S_3 layer, to compare with those of the device without remaining In_2S_3 layer, and it can be seen that the V_{oc} of the device with 5-nm-thick remaining In_2S_3 layer decreases. The efficiency decreases from 16.18% to 15.48%. Figure 10 shows the *J*–*V* curves of Zn(O,S)/In_2S_3/CZTSe devices with different band gaps of In_2S_3 layer band gap. To make the value of CBO between CZTSe layer and In_2S_3 layer varied in a range from 0 eV to +0.4 eV, the value of In_2S_3 layer band gap is changed from 2.4 eV to 2.8 eV. The performance parameters of the solar cells are almost unchanged at this time. However, the performance of the device deteriorates when the In_2S_3 layer band gap is below 2.4 eV due to the fact that the band alignment between CZTSe layer and In_2S_3 layer is cliff-like. So the optimal efficiency is 15.71% when the In_2S_3 band gap is 2.7 eV. And the parameters are listed in Table 3.

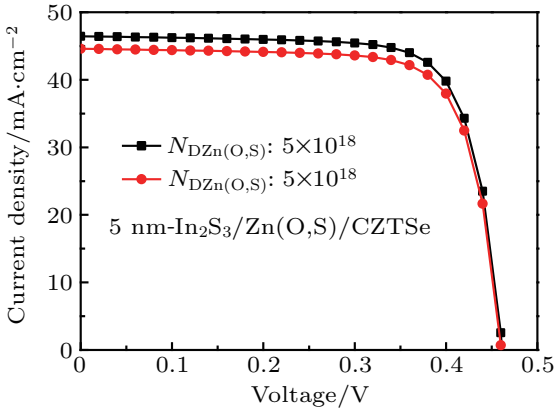


Fig. 9. The *J*–*V* curve of devices with and without 5-nm In_2S_3 layer.

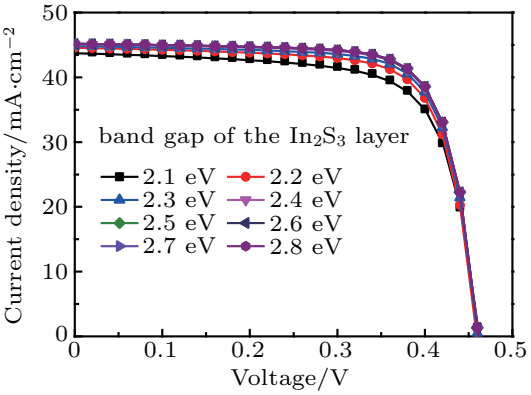


Fig. 10. The *J*–*V* curves of devices combined with In_2S_3 layer with different band gaps.

Table 3. Performances of Zn(O,S)/In_2S_3/CZTSe devices with 2.7-eV band gap In_2S_3 layer.

χ_e/eV	J_{sc}/(mA/cm^2)	V_{oc}/mV	FF/%	Efficiency/%
4.05	45.2	460	75.4	15.71

Figure 11 shows *J*–*V* curves of CZTSe devices in different buffer conditions, which are, respectively, for the following cases: $N_D = 5\times10^{17}$ cm^{-3} without In_2S_3 layer, $N_D =$

5×10^{18} cm^{-3} with In_2S_3 diffusing into the Zn(O,S) layer completely by annealing treatment, and $N_D = 5 \times 10^{18}$ cm^{-3} with 5-nm-thick In_2S_3 layer remaining on the top of Zn(O,S) layer or CZTSe layer. The detailed parameters are listed in Table 4, indicating that the device efficiency increases to 16.18% when the N_D is improved by In_2S_3 doping. The device performance becomes slightly worse when ultrathin In_2S_3 layer remains on the top of Zn(O,S) layer or CZTSe layer, while the parameters are still better than those without In_2S_3 layer due to the lower N_D in Zn(O,S) layer. Therefore, to achieve optimal device performance, the thickness of In_2S_3 layer should be very thin.

In summary, we have analyzed the performance of Zn(O,S)/CZTSe device from the perspective of band structure and carrier concentration by numerical simulation. The band alignment between Zn(O,S) layer and CZTSe layer is +0.2 eV and the carrier concentration of Zn(O,S) layer is improved by In_2S_3 doping. The efficiency of Zn(O,S)/CZTSe device is improved to 16.18%, when no In_2S_3 layer remains on CZTSe layer.

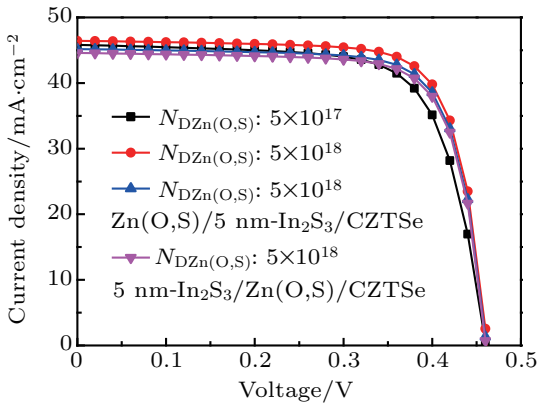


Fig. 11. *J–V* curves of devices for $N_D = 5 \times 10^{17}$ cm^{-3}, $N_D = 5 \times 10^{18}$ cm^{-3} without In_2S_3 layer, $N_D = 5 \times 10^{18}$ cm^{-3} with 5-nm-thick In_2S_3 layer remaining on Zn(O,S) layer, $N_D = 5 \times 10^{18}$ cm^{-3} with 5-nm-thick In_2S_3 layer remaining on CZTSe layer.

Table 4. Performances of devices for $N_D = 5 \times 10^{17}$ cm^{-3}, $N_D = 5 \times 10^{18}$ cm^{-3} without remaining In_2S_3 layer, $N_D = 5 \times 10^{18}$ cm^{-3} with 5-nm-thick In_2S_3 layer remaining on Zn(O,S) layer, $N_D = 5 \times 10^{18}$ cm^{-3} with 5-nm-thick In_2S_3 layer remaining on CZTSe layer.

Carrier concentration/cm^{-3}	In_2S_3 layer thickness/nm	J_{sc}/(mA/cm^2)	V_{oc}/mV	FF/%	Efficiency/%
$N_D = 5 \times 10^{17}$ cm^{-3}	0	45.8	460	70.8	14.93
$N_D = 5 \times 10^{18}$ cm^{-3}	0	46.4	462	75.5	16.18
$N_D = 5 \times 10^{18}$ cm^{-3} on Zn(O,S) layer	5	44.6	460	75.4	15.48
$N_D = 5 \times 10^{18}$ cm^{-3} on CZTSe layer	5	45.2	460	75.4	15.71

4. Conclusions

In this study, the Zn(O,S)/CZTSe solar cell performance is simulated and studied by using the wxAMPS software. To achieve the optimal performance, the S/(S + O) ratio in Zn(O,S), Zn(O,S) thickness, and carrier concentration are discussed. By numerical simulation, the optimum S fraction is about 0.7, here the value of CBO in the Zn(O,S)/CZTSe interface is about +0.2 eV. The CBO is in a range of 0 eV–0.4 eV as S/(S + O) = 0.6–0.8 in Zn(O,S). Meanwhile, the In_2S_3/Zn(O,S) double buffer layer is innovatively induced into the CZTSe device. The carrier concentration of the Zn(O,S) layer is improved by employing the In_2S_3/Zn(O,S) double buffer layer on CZTSe absorber layer upon annealing treatment. The device efficiency increases to 16.18% when the carrier concentration of Zn(O,S) layer is improved without any remaining In_2S_3. The efficiency of Zn(O,S)/5 nm-In_2S_3/CZTSe and 5 nm-In_2S_3/Zn(O,S) /CZTSe devices decrease to 15.71% and 15.48%, respectively. However, they are still higher than that of device without In_2S_3 layer (14.93%). These promising results indicate that the performance of Zn(O,S)/CZTSe device has great potential improvement and they provide guidance for further study of CZTSe solar cells.

References

[1] Li J, Kim S, Nam D, Liu X, Kim J, Cheong H, Liu W, Li H, Sun Y and Zhang Y 2017 *Sol. Energy Mater. Sol. Cells* **159** 447
[2] Polizzotti A, Repins I L, Noufi R, Wei S H and Mitzi D B 2013 *Energy Environ. Sci.* **6** 3171
[3] Mitzi D B, Gunawan O, Todorov T K, Wang K and Guha S 2011 *Sol. Energy Mater. Sol. Cells* **95** 1421
[4] Walsh A, Chen S, Wei S H and Gong X G 2012 *Adv. Energy Mater.* **2** 400
[5] Barkhouse D, Aaron R, Gunawan O, Gokmen T, Todorov T K and Mitzi D B 2012 *Prog. Photovoltaics Res. Appl.* **20** 6
[6] Bag S, Gunawan O, Gokmen T, Zhu Y, Todorov T K and Mitzi D B 2012 *Energy Environ. Sci.* **5** 7060
[7] Gao S, Jiang Z, Wu L, Ao J, Zeng Y, Sun Y and Zhang Y 2018 *Chin. Phys. B* **27** 018803
[8] Wang W, Winkler M T, Gunawan O, Gokmen T, Todorov T K, Zhu Y and Mitzi D B 2014 *Adv. Energy Mater.* **4** 1301465
[9] Lee Y S, Gershon T, Gunawan O, Todorov T K, Gokmen T, Virgus Y and Guha S 2015 *Adv. Energy Mater.* **5** 1401372
[10] Klenk R, Steigert A, Rissom T, Greiner D, Kaufmann C A, Unold T and Lux-Steiner M C 2014 *Prog. Photovoltaics Res. Appl.* **22** 161
[11] Gautron E, Buffière M, Harel S, Assmann L, Arzel L, Brohan L, Kessler J and Barreau N 2013 *Thin Solid Films* **535** 175
[12] Yagioka T and Nakada T 2009 *Appl. Phys. Express* **2** 072201
[13] Meyer B K, Polity A, Farangis B, He Y, Hasselkamp D and Wang C 2004 *Appl. Phys. Lett.* **85** 4929
[14] Chua R H, Li X, Walter T, The L K, Hahn T, Hergert F and Wong L H 2016 *Appl. Phys. Lett.* **108** 043505
[15] Grenet L, Grondin P, Coumert K, Karst N, Emieux F, Roux F, Fillon R, Altamura G, Fournier H, Faucher, P and Perraud S 2014 *Thin Solid Films* **564** 375
[16] Neuschitzer M, Lienau K, Guc M, Barrio L C, Haass S, Prieto J M and Izquierdo-Roca 2016 *J. Phys. D: Appl. Phys.* **49** 125602

[17] Li J, Liu X, Liu W, Wu L, Ge B, Lin S, Gao S, Zhou Z, Liu F, Sun Y, Ao J, Zhu H, Mai Y and Zhang Y 2017 *Sol. RRL.* **1** 1700075
[18] Hsieh T M, Lue S J, Ao J, Sun Y, Feng W S and Chang L B 2014 *J. Power Sources* **246** 443
[19] Steirer K X, Garris R L, Li J V, Dzara M J, Ndione P F, Ramanathan K, Repins I, Teeter G and Perkins C L 2015 *Phys. Chem. Chem. Phys.* **17** 15355
[20] Palimar S, Bangera K V and Shivakumar G K 2013 *Appl. Nanosci.* **3** 549
[21] Llican S, Caglar Y, Caglar M and Demirci B 2008 *J. Optoelectron. Adv. Mater.* **10** 2592
[22] Pham A T T, Ta H K T, Liu Y R, Aminzare M, Wong D P, Nguyen T H, Pham N K, Le T B N, Seetawan T, Ju H, Cho S, Chen K H, Tran V C and Phan T B 2018 *J. Alloys Compd.* **747** 156
[23] Benramache S, Benhaoua B and Bentrah H 2013 *Nanostrut. Chem.* **3** 54
[24] Gonçalves G, Elangovan E, Barquinha P, Pereira L, Martins R and Fortunato E 2007 *Thin Solid Films* **515** 8562
[25] Jani M, Raval D, Pati R K, Mukhopadhyay I and Ray A 2018 *Bull. Mater. Sci.* **41** 22
[26] Kim J, Hiroi H, Todorov T K, Gunawan O, Kuwahara M, Gokmen T, Nair D, Hopstaken M, Shin B, Lee Y S, Wang W, Sugimoto H and Mitzi D B 2014 *Adv. Mater.* **26** 7427
[27] Jiang F, Ozaki C, Guna wan, Harada T, Tang Z, Minemoto T, Nose Y and Ikeda S 2016 *Chem. Mater.* **28** 3283
[28] Liu Y, Sun Y and Rockett A 2012 *Sol. Energy Mater. Sol. Cells* **98** 124
[29] Omer and Mohamed B 2015 *Chin. Phys. Lett.* **32** 088801
[30] Sharbati S, Keshmiri S H, McGoffin J T and Geisthardt R 2015 *Appl. Phys. A* **118** 1259
[31] Persson C, Platzer-Bjorkman C, Malmstrom J, Torndahl T and Edoff M 2006 *Phys. Rev. Lett.* **97** 46403
[32] Grimm A, Kieven D, Klenk R, Lauermann I, Neisser A, Niesen T and Palm J 2011 *Thin Solid Films* **520** 1330
[33] Huang T J, Yin X, Qi G and Gong H 2014 *Phys. Status Solidi RRL.* **08** 735
[34] Minemoto T, Matsui T, Takakura H, Hamakawa Y, Negami T, Hashimoto Y and Kitagawa M 2001 *Sol. Energy Mater. Sol. Cells* **67** 83
[35] Barreau N, Bernede J C, Marsillac S and Mokrani A 2002 *J. Crystal Growth* **235** 439
[36] Revathi N, Prathap P, Subbaiah Y P V and Ramakrishna Reddy K T 2008 *J. Phys. D: Appl. Phys.* **41** 155404
[37] Saadallah F, Jebbari N, Kammoun N and Yacoubi N 2011 *Int. J. Photoenergy* 1–4
[38] Khoshsirat N and Md Yunus N A 2016 *J. Electron. Mater.* **45** 5721